Studies on Pyrene and Perylene Derivatives upon Oxidation and Application to a Higher Analogue

Akinobu Matsumoto, Mitsuharu Suzuki, Hironobu Hayashi, Daiki Kuzuhara,[†]
Junpei Yuasa,[††] Tsuyoshi Kawai, Naoki Aratani,* and Hiroko Yamada*

Graduate School of Materials Science, Nara Institute of Science and Technology (NAIST),
8916-5 Takayama-cho, Ikoma, Nara 630-0192

E-mail: aratani@ms.naist.jp, hyamada@ms.naist.jp

Naoki Aratani
Naoki Aratani was born in 1975 in Nagoya, Japan. He received his Ph.D. degree in 2005 from Kyoto University, under the guidance of Prof. Atsuhiro Osuka. In 2003, he started an academic career as an Assistant Professor in the Graduate School of Science, Kyoto University. In 2006–2007, he joined Prof. Omar M. Yaghi's group as a visiting scientist at the UCLA, studying porous crystalline materials. In 2009–2013, he was a researcher of PRESTO, JST. In 2012, he moved to Nara Institute of Science and Technology as an Associate Professor. His research interests focus on the creation of novel π-functional molecules.

Hiroko Yamada
Hiroko Yamada received her Ph.D. degree (Science) in 1992 from Kyoto University. Since 2008, she is an associate professor at Ehime University, then moved to NAIST in 2011. She was promoted to a full professor at NAIST in 2012. From 2007 to 2010, she was a researcher of PRESTO, JST, and then a group leader of CREST project (2010–2016), JST, on "Construction of organic thin-film solar cells with innovative solution-processible organic materials". Her current research focuses on the development of functional organic materials including solution-processable molecular materials for organic electronics applications, large acenes and bottom-up synthesis of graphene nanoribbons.

Abstract

The structure and electronic features of neutral and positively charged pyrene and perylene derivatives were explored. The radical cation of 1,3,6,8-tetraarylpyrene **1** was examined by ESR, UV–vis–NIR spectroscopy and theoretical calculations. The addition of 2 equiv of oxidant to **1** resulted in the formation of dication $\mathbf{1}^{2+}$. The single-crystal X-ray structure of $\mathbf{1}^{2+}$ proved that the aromatic part relocates from biphenyl unit to naphthyl unit upon $2e^-$ oxidation of **1**. We have also investigated the oxidation processes of 3,9-diarylperylene **2** and 3,10-diarylperylene **3**. The radical cations of $\mathbf{2}^{\cdot+}$ and $\mathbf{3}^{\cdot+}$ showed ESR signals and the spin densities were proven to delocalize at 3,4,9,10-positions. In the case of doubly charged 3,9-diarylperylene, we could find the anthracene structure in the core, while the phenanthrene skeleton appeared in two-electron oxi-

dized 3,10-diarylperylene. Finally we validated this phenomenon to apply for the higher analogue terrylene, discovering its large aromaticity relocation upon the $2e^-$ oxidation.

1. Introduction

While polycyclic aromatic hydrocarbons (PAHs) and their various derivatives are very common in chemistry, their cationic and dicationic species are not properly investigated under normal experimental conditions due to their remarkable reactivity, so it is rather difficult to obtain the structural information especially in their solid state. Under special conditions, Olah has achieved the generation and characterization of a series of charged PAHs in super acid.[1] In general, however, the oxidation of the unsubstituted PAHs having appropriate oxidation potential typically results in the formation of directly linked PAH oligomers.[2–9] In case of pyrene, the oxidation gives a 1,1′-linked pyrene dimer (Scheme 1).[10,11] In order to investigate their isolated cationic species, it is necessary to "cap" some of the most reactive positions by the substituents to prevent (random) oligomerization.[12]
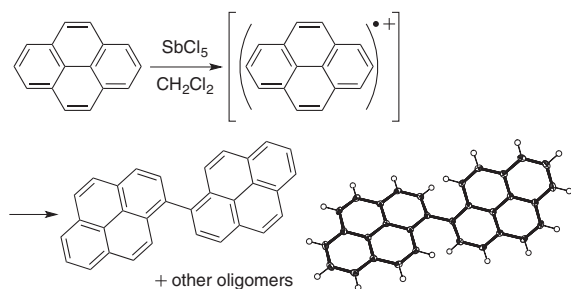
Scheme 1. Oxidative oligomerization of an intact pyrene and single-crystal X-ray structure of dimer.[10]
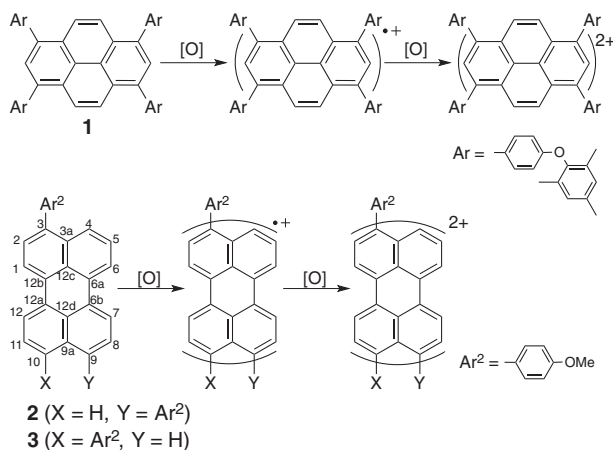
Scheme 2. Oxidation of pyrene derivative **1** and perylene derivatives **2** and **3**. The carbon designation for perylene is described.

In these decades, considerable efforts have been made for the characterization of radical cations and dications with long lifetimes and some of them have been isolable.[13–25] There have been deep discussions on the stability of dicationic species of PAHs.[26] As an interesting example, Bettinger et al. have discovered the fact that dications of higher linear acenes are formed more easily with growing size in sulfuric acid.[27] A computational analysis of anthracene concluded that the doubly charged system could be drawn with two Clar sextets.[28–32]

In our previous communications, we reported that the sterically hindered pyrenes and perylenes could be oxidized with SbCl$_5$ to give persistent cations and dications (Scheme 2).[33] The aromatic site of the dications relocates from the biphenyl to the naphthalene for pyrene, and from the naphthalene to the anthracene or phenanthrene for perylene, respectively, judging from the structures determined by the single-crystal X-ray analysis for the first time.

In this article, we have analyzed these oxidation processes of the pyrene and perylene derivatives in detail via the corresponding radical cations both experimentally and theoretically (Scheme 2). Especially, the formation of discrete radical cationic state of those compounds was confirmed by means of an ESR technique and analyzed by theoretical calculations. In addition, we validated the aromaticity relocation phenomena of the higher analogue terrylene upon the 2e$^-$ oxidation.

2. Experimental

Synthetic procedures for **1**, **2**, and **3** were reported in previous communications.[33] ^{1}H NMR (400 MHz) and ^{13}C NMR (100 MHz and 150 MHz) spectra were recorded with JEOL JNM-ECX 400 and JEOL JNM-ECP 400 and JEOL JNM-ECA 600 spectrometers at ambient temperature by using tetramethylsilane as an internal standard. X-ray crystallographic data were recorded at 90 K on a Bruker APEX II X-ray diffractometer equipped with a large area CCD detector by using graphite monochromated Mo-Kα radiation ($\lambda = 0.71073$ Å). UV/Vis absorption spectra were measured with a JASCO UV/Vis/NIR spectrophotometer V-670. Fluorescence spectra were measured with a JASCO FP-6600 spectrophotometer. Fluorescence quantum yields were measured on a Hamamatsu Absolute PL Quantum Yield Measurement System C9920-02. CV measurements were conducted in a solution of 0.1 M TBAPF$_6$ in dry dichloromethane with a scan rate of 100 mV/s at room temperature in an argon-filled cell. A glassy carbon electrode and a Pt wire were used as a working and a counter electrode, respectively. An Ag/Ag$^+$ electrode was used as reference electrodes, which were normalized with the half-wave potential of ferrocene/ferrocenium$^+$ (Fc/Fc$^+$) redox couple. ESR spectra were measured with JEOL JES-FA100N. For spectral measurements, spectral-grade toluene was purchased from Nacalai Tesque.

Density functional theory (DFT) calculations were employed with the Gaussian 09 package.[34] Ground states of neutral state were calculated at the B3LYP level of theory with basis set 6-31G(d), and radical cation and dication states were calculated by the combination of global hybrid functionals with exact-exchange admixtures of 35% (BLYP35) with basis set SVP with CPCM solvent model implementations in MeCN (see discussion).[35] The calculated absorptions were computed at the time-dependent (TD)-DFT level with the same functional and solvent. NICS(0) values were calculated at the B3LYP/6-311++G(2d,p) level using the optimized structure and the standard GIAO procedure.

3. Results and Discussion

Pyrene Case. Pyrene derivatives are in general highly emissive and many applications are found in optical sensors, non-linear optics, and light emitting diodes.[36] Electrophilic substitution of pyrene at the 1-, 3-, 6-, and 8-positions and subsequent transformation has led to enormous organic molecules that have been used in electronic and optoelectronic devices.[37] The pyrene radical cation is normally highly reactive and its characterization is difficult. The oxidation of pyrene is usually irreversible at room temperature in conventional solvent.

The oxidation of the unsubstituted pyrene results in the formation of 1,1′-linked oligopyrenes as mentioned above.[2,11] Rathore et al. successfully isolated the radical cation of 1,3,6,8-tetraisopropylpyrene.[38] This compound showed a reversible oxidation wave at +0.98 V (versus SCE) and an intense absorption band of the pyrene radical cation at 494 nm. Alkylpyrene dications by two-electron oxidation with SbF$_5$/SO$_2$ClF were observed in low-temperature ^{13}C NMR.[39] Introduction of diphenylamino groups at 2- and 7-positions enable the generation of stable dicationic species but the positive charges are outside of the pyrene core.[40] Its anion version was achieved by the diborylpyrene.[41]

A well-known problem of pyrene derivatives is that their emission in the solid state is effectively quenched because
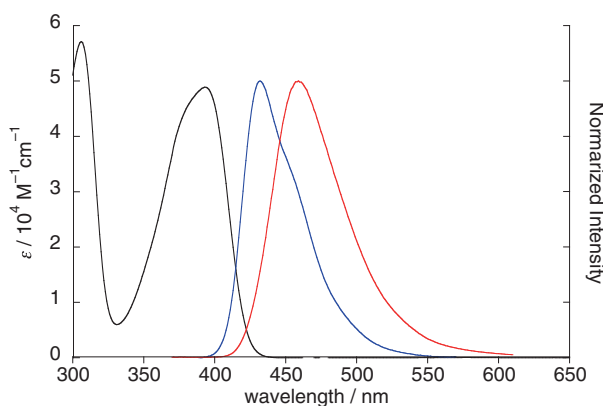
Figure 1. UV–vis absorption (black) and fluorescence spectra of **1** in toluene (blue) and in the solid (red).

Figure 2. CV of **1** in 0.1 M TBAPF$_6$/CH$_2$Cl$_2$ at 100 mVs^{-1}.

Figure 3. MO diagrams of pyrene and **1′** (Mesityl groups of **1** were replaced by methyl groups).

of the formation of self-aggregation via π-stacking.[42] Many research groups have attempted to enhance the emission from the pyrene core in the solid state by modifying the molecular structures.[43] Sterically congested mesityl substituents can prevent undesirable face-to-face π-stacking, so that self-quenching is impeded to permit efficient emission.[44] In reverse, aggregation-induced emission (AIE) is one of the most elegant strategies for making solid-state pyrenes emissive.[45]

We have investigated the effect of bulky substituents at the periphery of the pyrene by 1,3,6,8-tetrakis(naphthalen-1-yl)-pyrene.[33a] In addition to the facile synthetic accessibility by Suzuki–Miyaura cross-coupling, the bulky aryl rings were a priori anticipated to contribute to the improvement of the redox stability of pyrene derivatives (Scheme 2). 1,3,6,8-Tetrakis(4-mesityloxyphenyl)pyrene (**1**) was also synthesized by the standard Suzuki–Miyaura cross-coupling between 2-(4-chlorophenoxy)-1,3,5-trimethylbenzene and 1,3,6,8-tetraborylpyrene.[33b] The pyrene core unit in the solid state is perfectly planar with the mean-plane deviation of 0.046 Å and does not form face-to-face stacking owing to the peripheral aryl groups.[33b,46] The center-to-center distance between the pyrene cores in the solid state is about 7.27 Å, suggesting negligible interaction between the pyrene units. The attached phenyl units in **1** are relatively coplanar to the pyrene plane (49° and 52°).

UV–vis absorption and fluorescence spectra of **1** in toluene are shown in Figure 1. Compared to the pristine pyrene ($\lambda_{max} = 337$ nm), compound **1** exhibits red-shifted and broader absorption ($\lambda_{max} = 393$ nm), suggesting the electronic communication between the pyrene and aryl units. Fluorescence quantum yield of **1** in toluene has been also measured to be 9%. The fluorescence peak wavelength is 432 nm. To further investigate the physical properties, the fluorescence spectrum and quantum yield of the single crystals of **1** have been measured (Figure 1). The fluorescence peak wavelength of the crystalline state is 459 nm, which is longer than those observed in solution, indicating packing effects of **1**. The florescence quantum yield of **1** in the solid state (22%) is higher than that in solution, thus **1** exhibits AIE.[45]

Figure 2 shows the cyclic voltammetry (CV) of **1** in CH$_2$Cl$_2$. Compound **1** shows reversible oxidative waves at +0.5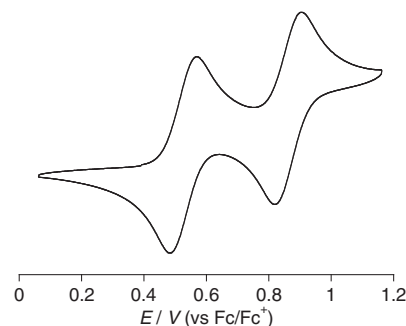3 and +0.86 V (versus Fc/Fc$^+$). Compared to the first oxidation potential of the pristine pyrene, that of compound **1** shifted to a lower potential. To understand its electronic features, MO calculations of the model compound **1′** (mesityl groups were replaced by methyl groups) were performed (Figure 3). The highest occupied molecular orbital (HOMO) of **1** is mainly located over the π-conjugated core skeleton but delocalized also to the aryl-substituents to some extent. The energy levels of the HOMO and the lowest-unoccupied molecular orbital (LUMO) of **1** were calculated to be −4.74 eV and −1.48 eV, respectively.
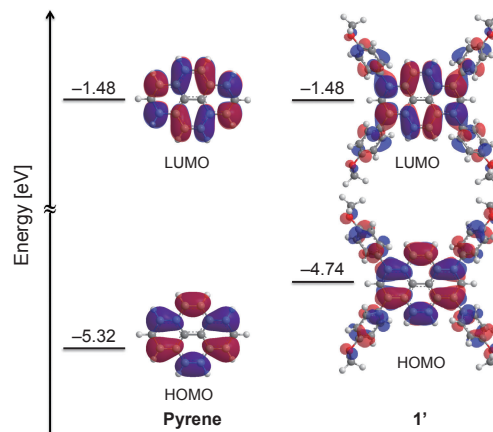
The reversible oxidation found for **1** encouraged us to investigate the ability of **1** for the generation of the stable cationic and dicationic species.[47] Generation of the cationic species of **1** was carried out with NOSbF$_6$, which is known as a powerful one-electron oxidation agent. **1** was subjected to stepwise oxidations with NOSbF$_6$ (1 or 2 equiv) in CH$_2$Cl$_2$/CH$_3$CN. Although the oxidation of parent pyrene with the oxidant immediately forms its oligomers as mentioned above (within 5 min), 60% of absorption of **1**$^{•+}$ remains even after 24 h under ambient conditions. The UV–vis–NIR absorption spectra are shown in Figure 4. After addition of 1 eq of NOSbF$_6$ to **1**, the intense band at 306 nm and 393 nm decreased, whereas new bands in visible region at 626 nm and the NIR region at 926 nm arose. The absorption spectrum is practically the same as that of the electro-chemically oxidized **1** at +0.58 V (versus Fc/Fc$^+$).

The formation of the radical cation was also confirmed by ESR spectroscopy (Figure 5). The radical cation of **1**$^{•+}$ exhibited a single-line ESR signal at $g = 2.0024$, which corresponds
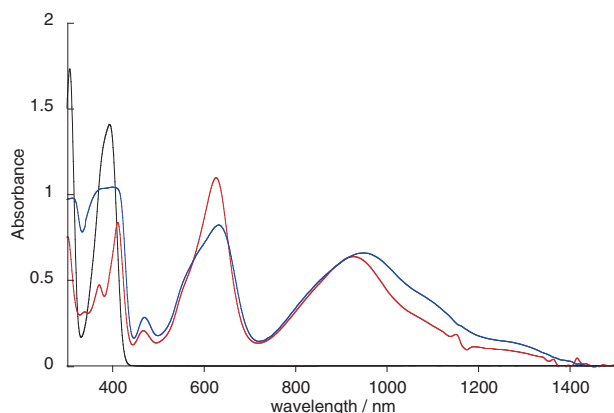
Figure 4. UV–vis–NIR absorption spectra of **1** (black), **1**[•+] (red) ($3.0 \times 10^{-5}\,M^{-1}$) formed under the oxidation with 1 equiv of $NOSbF_6$ in CH_2Cl_2/CH_3CN at room temperature, and electrochemically oxidized **1** at $+0.58\,V$ (blue).
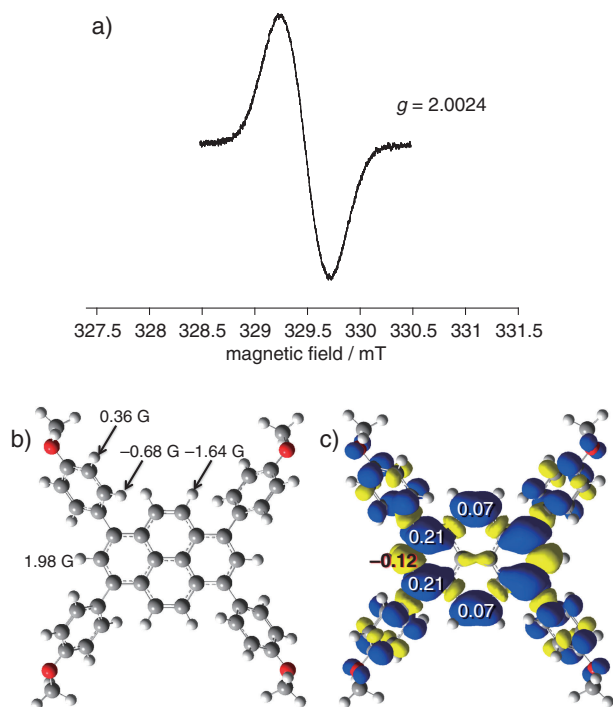

Figure 5. a) ESR spectrum of **1**[•+], b) hyperfine coupling constants estimated by DFT calculations at the UBLYP35/SVP (with CPCM solvent model implementations in MeCN), and c) spin density of **1**[•+] by the same calculations. See text.

to a general organic free radical compound. Since the hyperfine coupling constants (hfccs) were not clearly observed, it is considered that the electronic correlation of radical cations is very fast. The signal of **1**[•+] in ESR spectrum is attributed to four hydrogen positions (Figure 5b).

Computed spin densities showed that the unpaired electrons were delocalized over the aromatic skeleton. According to the spin density calculations, **1**[•+] has the highest spin densities of 0.21 on C1, C3, C6, and C8 substituted with aryl groups (Figure 5c). Thus the aryl groups are indeed contributing as steric protection to the radical.
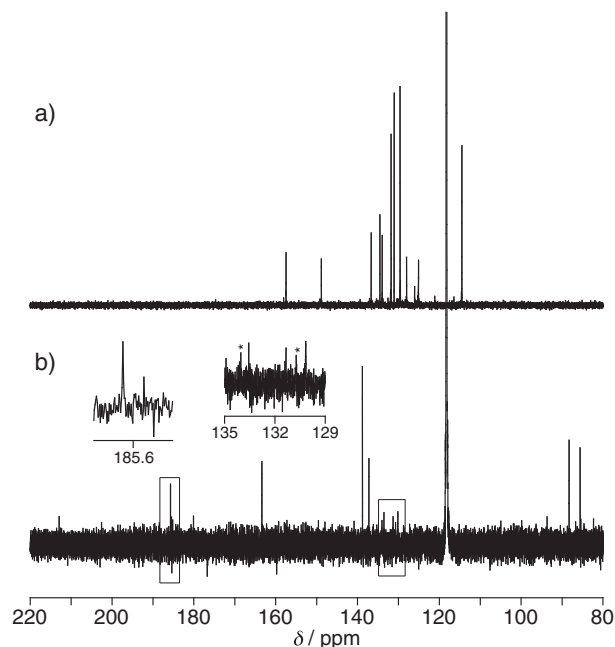

Figure 6. ^{13}C NMR spectra of a) neutral **1** in $CDCl_3$ at room temperature and b) dication **1**[2+] in CD_3CN at $-40\,°C$.

Upon further addition of $NOSbF_6$ (totally 2 equiv), **1**[•+] was oxidized to the dicationic species **1**[2+], resulting in the appearance of visible band at 621 nm, and the disappearance of the ESR signals. Interestingly, the lifetime of dicationic species is even longer than that of cationic one, checked by UV–vis absorption spectral change (only 26% degradation) after 24 h under ambient conditions. The ground state of dicationic species was predicted to be singlet rather than triplet by DFT calculations with energy difference of 15.6 kcal/mol.

We have measured ^{13}C NMR spectrum of **1**[2+] at $-40\,°C$ in CD_3CN as shown in Figure 6 along with the spectrum for the neutral **1**. All 13 non-equivalent aromatic carbons were observed at $\delta = 212.94, 185.71, 185.49, 180.09, 163.37, 138.80, 137.24, 133.57, 131.34, 130.17, 93.68, 88.30,$ and 85.58 ppm.

Conventionally, DFT calculations at the (U)B3LYP/6-31G(d) level were conducted to simulate UV–vis absorption spectra of charged species or to provide a singly occupied molecular orbital. However, it has been demonstrated by multiple research groups that (U)B3LYP over-delocalizes the charge in π-conjugated systems.[35] Therefore, the calculation for **1**[•+] was performed by time-dependent density functional theory (TD-DFT) at the (U)BLYP35/SVP (with CPCM solvent model implementations in MeCN)[35] using the Gaussian 09 package.

The calculation accuracy was confirmed by comparison between the absorptions calculated with (U)B3LYP/6-31G(d) and (U)BLYP35/SVP (with CPCM solvent model implementations in MeCN) (Figure 7). The fact that the B3LYP (blue bars) overestimates the charge delocalization was indicated by the calculated absorptions for both **1**[•+] and **1**[2+]. Eventually, the absorption with (U)BLYP35/SVP (red bars) better agrees with the experimental data than that with (U)B3LYP/6-31G(d).

We have succeeded to make single crystals of **1**[2+].[33b,48] After considerable attempts, we found the crystallization conditions: to a solution of **1** in anhydrous dichloromethane and hexane
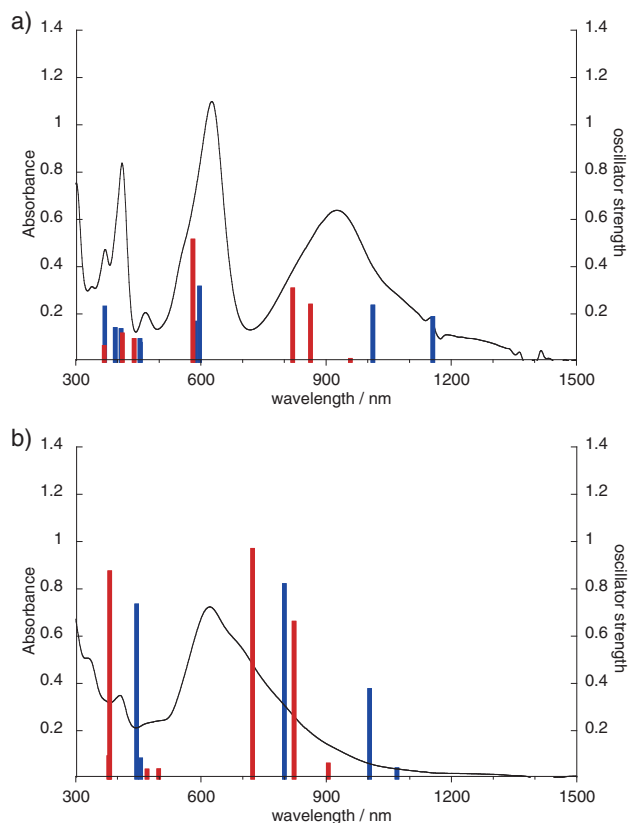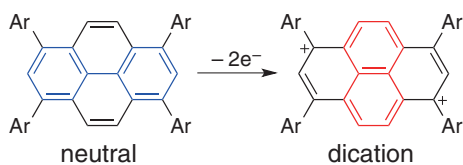
Figure 8. X-ray single-crystal structure of 3,9-dibromoperylene. Thermal ellipsoids are scaled at 50% probability.

(rings having larger HOMA values) relocates from the biphenyl part into the naphthalene unit upon the two-electron oxidation (Scheme 3). These experimental results show a correlation with theoretical calculations.[33a] The nucleus independent chemical shift (NICS)[51] is another aromaticity index. Although the NICS values for charged systems tend to be high due to the electron deficient situation,[52] the switch of the magnetic properties is observed from neutral **1** to dication **1**$^{2+}$.

Perylene's Case. Perylene derivatives are also very common in chemistry. While their isolated anionic and dianionic species are practically available in experimental conditions,[53] their cationic and dicationic species are unstable due to their high reactivity.[54] The oxidation of the perylene derivative having an imino bridge at a bay area results in the formation of directly linked dimers.[6] Therefore, in order to investigate the isolated cationic species, it is necessary to cap the most reactive positions by the substituents as well.

Electrophilic substitution of perylene at the 3-, 4-, 9-, and 10-positions and subsequent transformation have led to numerous compounds.[55] Alkylperylene dications by two-electron oxidation with SbF$_5$/SO$_2$ClF were observed in low-temperature ^{13}C NMR.[56]

Synthesis of 3,9- or 3,10-dibromoperylene was reported in the literature.[57] Nevertheless, 3,9- and 3,10-dibromoperylenes were not able to be easily separated in our hands. R_f values on silica gel and retention times on GPC and Buckyprep column are all identical. Beside, the identical ^{1}H NMR, UV–vis absorption and mass spectra hamper the determination of the isomers and their purity. Finally repetitive recrystallization from aniline/nitrobenzene (1/1 v/v) gave pure 3,9-dibromoperylene[57] and the structure was characterized by single-crystal X-ray diffraction analysis (Figure 8),[58] then the filtrate was recrystallized from aniline/toluene (5/3 v/v) to afford pure 3,10-dibromoperylene. Melting points for these two compounds are different.[33b]

3,9-Diarylperylene **2** was synthesized by Suzuki–Miyaura cross-coupling between 4-borylanisole and 3,9-dibromoperylene. **2** and **3** also demonstrated identical ^{1}H NMR spectra. Therefore, the structures of **2**[59] and **3**[60] were determined by single-crystal X-ray diffraction analysis.[33b] Each perylene core unit in the solid state is perfectly planar with the mean-plane deviation of 0.041 Å and 0.036 Å, respectively and does not form face-to-face stacking owing to the peripheral aryl groups. The center-to-center distances between the perylene cores in the solid state of **2** and **3** are about 5.97 and 5.84 Å, respectively,

Figure 7. UV–vis–NIR absorption spectra of a) **1**$^{•+}$ and b) **1**$^{2+}$ (3.0×10^{-5} M^{-1}) formed under the oxidation with NOSbF$_6$ in CH$_2$Cl$_2$/CH$_3$CN at room temperature along with oscillator strengths calculated by (U)B3LYP/6-31G(d) (blue) and (U)BLYP35/SVP (with CPCM solvent model implementations in MeCN) (red).

Scheme 3. Schematic representation of the aromaticity relocation of pyrene **1** upon the two-electron oxidation.

was added SbCl$_5$ (excess) under an argon atmosphere at 5 °C. The crystal structure of **1**$^{2+}$·2(SbCl$_6$)$^-$ revealed that the counter anions are positioned above and below the pyrene plane. The dihedral angles of phenyl units in **1**$^{2+}$ are 41° and 42°. Compared to the neutral state, the phenyl groups tilted about 9°. Interestingly, the plane constructed from C1, C2, and C3 in **1**$^{2+}$ was twisted toward the planar central naphthalene core by 9°. The quinoidal contributions of mesityloxyphenyl groups are likely not negligible to stabilize dicationic state (Scheme 3).

The bond length alternations from **1** to **1**$^{2+}$ and the twist of the lateral 3C units should indicate the large change of its electronic system. To check their aromaticity of the neutral and charged species, we performed harmonic oscillator model of aromaticity (HOMA)[49] value estimation for **1** and **1**$^{2+}$ on the basis of crystal structures.[33b] By the electronic system rearrangement upon the two-electron oxidation, the bond lengths become rather close to naphthalene.[50] Thus the aromaticity of the pyrene
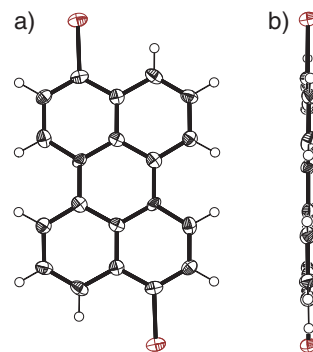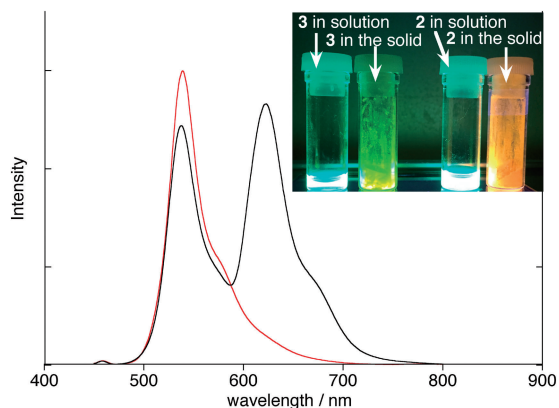
Figure 9. Fluorescence spectra of **2** (black) and **3** (red) in the solid-state. Inset: A photograph of **2** and **3** in solution and in the solid state under irradiation with a hand-held UV lamp (365 nm).

Figure 10. MO diagrams of perylenes **2** and **3**.

suggesting certain interaction between the perylene units. The phenyl units in **2** and **3** are relatively coplanar to the perylene plane (around 60°).

Compared to the pristine perylene ($\lambda_{max} = 439\,nm$), **2** and **3** exhibit red-shifted and broader absorption ($\lambda_{max} = 461$ and $462\,nm$, respectively), suggesting the electronic communication between the perylene and aryl units. Fluorescence quantum yields of **2** and **3** in toluene have been measured to be 85 and 95%, respectively. The fluorescence peak wavelengths are 485 and 487 nm. Thus, spectral characteristics of **2** and **3** in solution are also practically identical.

To further investigate the physical properties, the fluorescence spectra and fluorescence quantum yields in the solid state of **2** and **3** have been measured (Figure 9). The fluorescence peak wavelengths in the solid state are 538 nm and 623 nm for **2**, and 539 nm for **3**, both of which are longer than those observed in solution. However, the second peak (623 nm) for **2** would indicate excimer effects in the crystalline state, so that the solid-state properties are largely different. The florescence quantum yields of **2** and **3** in the solid state (44 and 15%) are lower than those in solution.

CV of **2** and **3** in CH_2Cl_2 show reversible oxidative waves at $+0.41$ and $+0.79\,V$ for **2**, and $+0.42$ and $+0.78\,V$ for **3** (vs Fc/Fc$^+$).[33b] Compared to the first oxidation potential of the pristine perylene ($0.54\,V$ vs Fc/Fc$^+$), those of compounds **2** and **3** shifted to a lower potential.

The generation of the cationic and dicationic species of **2** was carried out with NOSbF$_6$ (1 or 2 equiv) in CH_2Cl_2/CH_3CN. After addition of 1 equiv of NOSbF$_6$ to **2**, the intense band at 432 nm and 458 nm decreased, whereas new bands in visible region at 743 and 595 nm and the NIR region at 1002 nm arose. In the case of perylene, the oxidation with the same oxidant induces its degradation within 5 min, while a half of absorption of **2**$^{•+}$ remains after 24 h under ambient conditions. The absorption spectrum is practically the same as that of the electrochemically oxidized **2** at $+0.52\,V$ (vs Fc/Fc$^+$).[33b]

Addition of 1 eq of NOSbF$_6$ to **3** generated the intense band at 434 nm and 462 nm decreased, whereas new bands in the visible region at 714 nm and the NIR region at 969 nm arose. Almost half of the absorption of **3**$^{•+}$ remains after 24 h. This
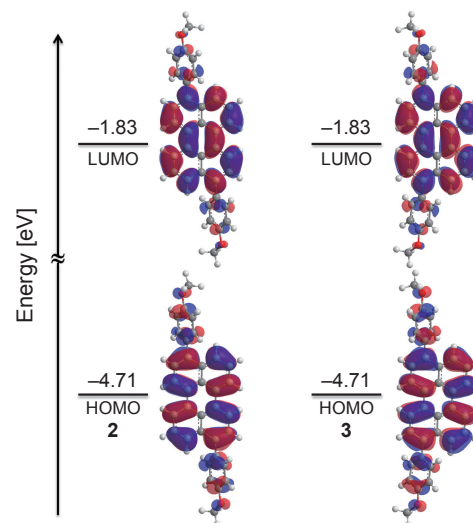
absorption spectrum is also the same as that of the electrochemically oxidized **3** at $+0.56\,V$ (versus Fc/Fc$^+$). The simulated absorptions are accordance with the observed data.

To understand their electronic features, MO calculations of the compounds **2** and **3** were performed by DFT at the B3LYP/6-31G(d) level (Figure 10). The HOMOs of **2** and **3** are located over the π-conjugated core skeleton but delocalized also to the aryl-substituents to some extent. The energy levels of the HOMOs and the LUMOs of neutral **2** and **3** were calculated to be both $-4.71\,eV$ and $-1.83\,eV$, respectively.

The formation of the radical cation was also confirmed by ESR spectroscopy (Figure 11). The radical cation of **2**$^{•+}$ exhibited an ESR signal at $g = 2.0023$, which corresponds to a general organic free radical compound. The signal of **2**$^{•+}$ is attributed to three kinds of hydrogen positions in the perylene skeleton. The hfccs were simulated from the observed spectrum and Gauss values calculated by DFT to be 4.10 (2H), 0.65 (4H), and 2.85 (4H) G with $\Delta H = 1.0\,G$ (Figures 11a and 11c). The radical cation of **3**$^{•+}$ exhibited an ESR signal at $g = 2.0019$. The signal of **3**$^{•+}$ is also attributed to three kinds of hydrogen positions in the core perylene, and the hfccs were simulated from the observed spectrum and calculated Gauss values to be 3.90 (2H), 0.65 (4H), and 2.85 (4H) G with $\Delta H = 1.1\,G$ (Figures 11b and 11e). Computed spin densities showed that the unpaired electrons were delocalized over the whole molecules. **2** and **3** have the highest spin densities on C3, C4, C9, and C10 (Figures 11d and 11f).

Upon further addition of NOSbF$_6$ (totally 2 eq), **2**$^{•+}$ was oxidized to form the dicationic species **2**$^{2+}$, resulting in the disappearance of the ESR signals. This indicates that the singlet state of **2**$^{2+}$ is more stable than its triplet state. The ground state of dicationic species of **2**$^{2+}$ was also predicted to be singlet by the DFT calculations with the energy gap of 12.1 kcal/mol. The lifetime of dicationic species is almost the same with that of the cation, checked by UV–vis absorption spectral change under ambient conditions.

By the electronic system rearrangement upon the oxidation, the bond lengths observed in single-crystal X-ray structure[33b,61] approach those of anthracene[62] (Figure 12). Here, the plane constructed from C1, C2, and C3 in **2**$^{2+}$ is twisted toward the planar
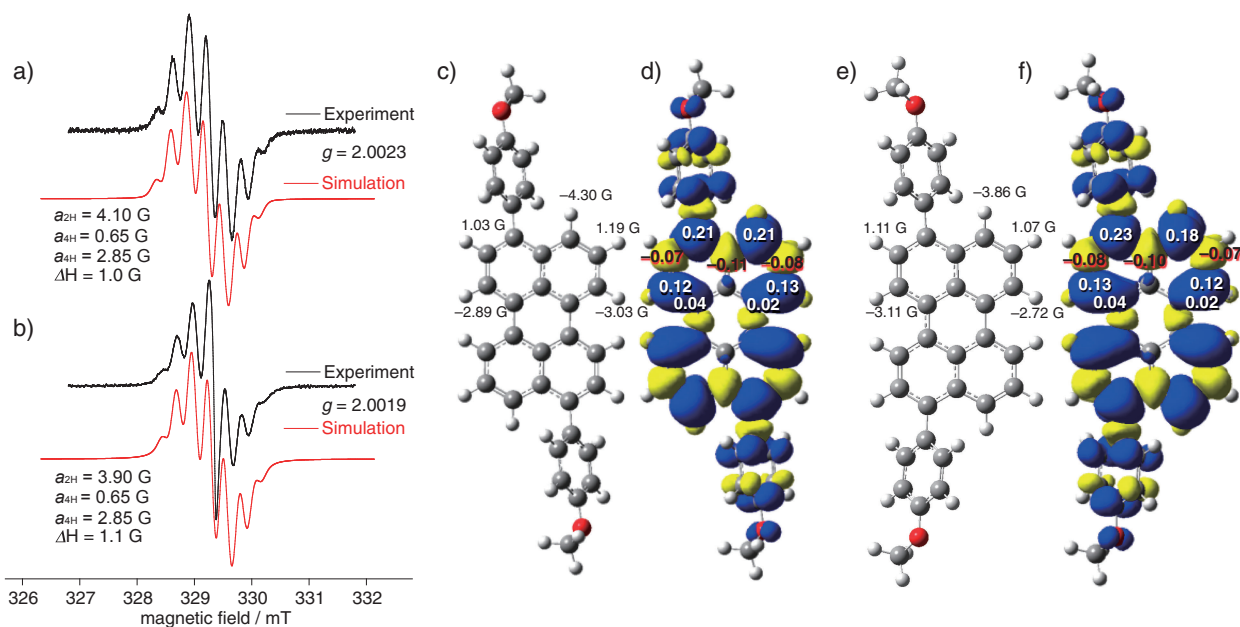
Figure 11. a) ESR spectra and simulations of a) $2^{•+}$ and b) $3^{•+}$, c) hyperfine coupling constants of $2^{•+}$, d) spin density of $2^{•+}$, e) hyperfine coupling constants of $3^{•+}$, and f) spin density of $3^{•+}$, by DFT calculations at the UBLYP35/SVP (with CPCM solvent model implementations in MeCN).
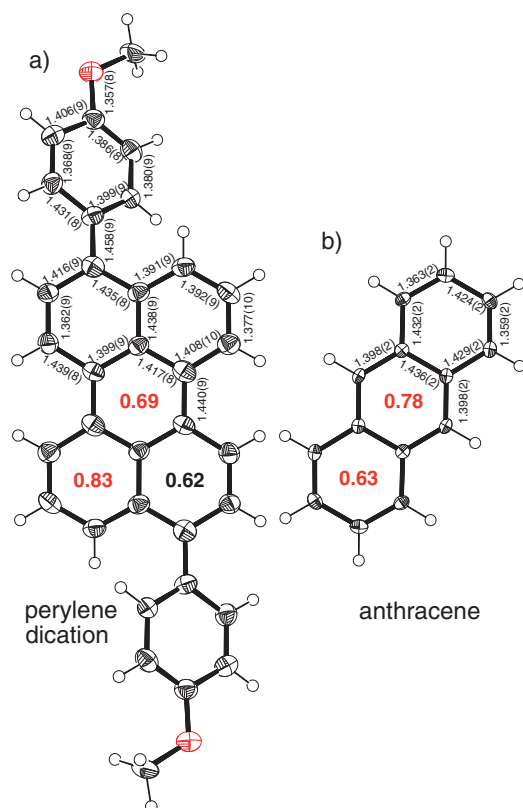

Figure 12. The bond lengths (Å) and the calculated HOMA values (bold) based on the single-crystal structures of a) 2^{2+} and b) neutral anthracene.[62]

central anthracene core by 10°. The aromaticity of the perylene (larger HOMA values) relocates from the (two) naphthalene parts into the anthracene unit upon the two-electron oxidation.

Further addition of NOSbF₆ (totally 2 equiv) to $3^{•+}$ resulted in the formation of the dicationic species 3^{2+}. The disappearance of the ESR signals indicate that the singlet state of 3^{2+} is more stable than its triplet state as well. The energy gap calculated was 21.2 kcal/mol. The lifetime is almost the same with that of the cation, a half of the absorption remains after 24 h.

In spite of many attempts, crystals of 3^{2+} suitable for X-ray measurement could not be obtained to date. Theoretical calculations for 3^{2+} predict similar behavior to 2^{2+}; the bond lengths approach those of phenanthrene (Figure 13).

Terrylene Case and More. Multiple experimental and theoretical evidence proved that the physical and chemical properties of the dicationic pyrene and perylenes were well-explained by Clar's aromatic π-sextet rule accompanying aromaticity relocation. To elucidate the scope in which this concept is applicable, we performed theoretical calculations of several larger PAHs upon the $2e^-$ oxidation. Among these, we found a pair of interesting examples, 3,12-bis(4-methoxyphenyl)terrylene **4** and its dication state.[63,64]

Terrylene, one of the oligorylene dyes (perylene, terrylene, quaterrylene, etc.), can be considered as a piece of armchair graphene nanoribbons (GNRs; $N = 5$)[65,66] (Figure 14). Well-defined GNRs are of great interest because it is possible to tailor the band gap to meet the needs of particular devices. Theoretically GNRs with an armchair orientation range from a small band gap to zero band-gap semiconductors, depending on their width N.[67]

The singlet state of 4^{2+} is calculated to be more stable than its triplet state by 17.6 kcal/mol. As the molecular size becomes larger from perylene to terrylene, the degree of change of HOMA values in naphthalene units upon the $2e^-$ oxidation becomes moderate (Figure 15). However, importantly, the benzene rings fusing naphthalene units drastically increase their aromaticity (HOMA: $0.09 \rightarrow 0.61$, NICS(0): $7.61 \rightarrow -3.04$)
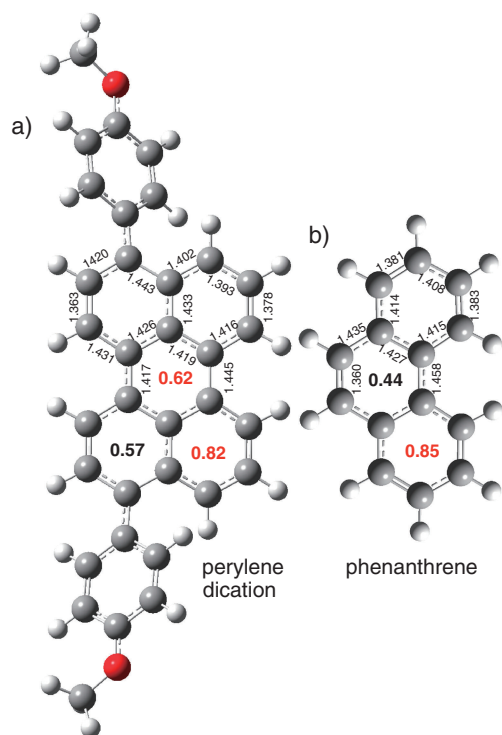
Figure 13. The bond lengths (Å) and the calculated HOMA values (bold) based on the optimized structures of a) 3^{2+} and b) phenanthrene.

Figure 14. Oligo- and polyrylene structures. The carbon designation is described in terrylene.

(Figures 15 and 16). Consequently the total aromatic structure of terrylene shifts towards that of picene by $2e^-$ oxidation (Scheme 4).

Inspired by these discussions, we would like to consider the electronic structure of neutral polyrylenes, since we have recently observed very unusual open-shell diradical character for long rylene molecules, which can be correlated to the potential metallic property of the infinite polyrylene ribbon.[68] Though the oligorylenes behave as connected naphthalenes (Figure 17a), it is predicted that the longer rylenes exhibit diradical character even in the neutral state.[69] Furthermore, early theoretical calculations have indicated the neutral polyrylene as either parallel polyacetylene chains (Figure 17b), or a planar poly(p-phenylene) bridged by double bonds (Figure 17c).[70,71] It is proved that the end groups or doping affect the whole electronic structure of the polyrylene.[72]
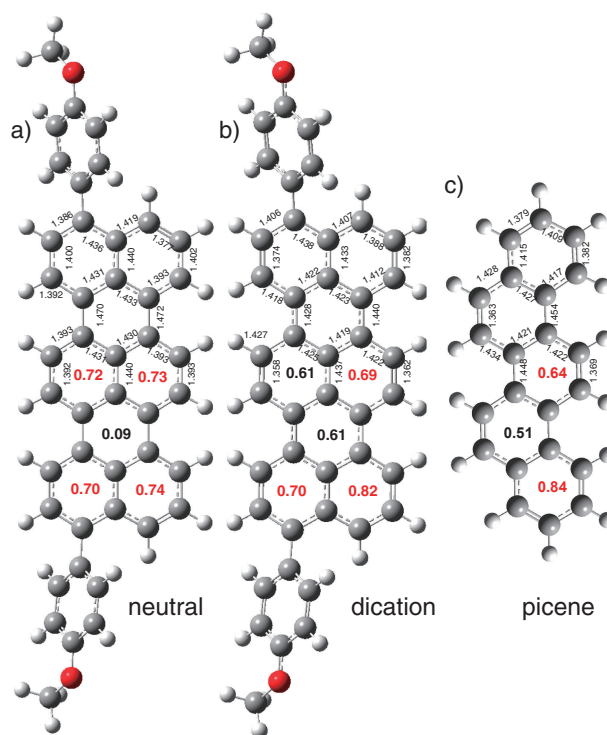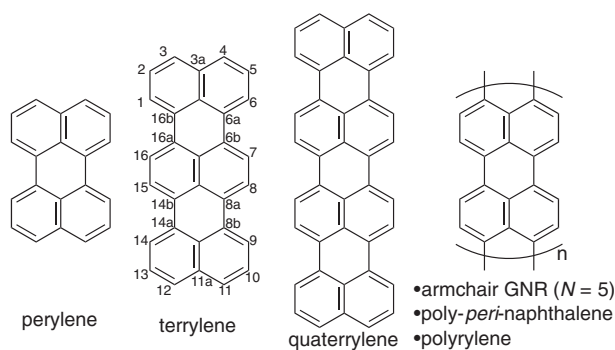

Figure 15. The bond lengths (Å) and the calculated HOMA values (bold) based on the optimized structures of a) terrylene **4**, b) terrylene dication 4^{2+}, and c) picene.
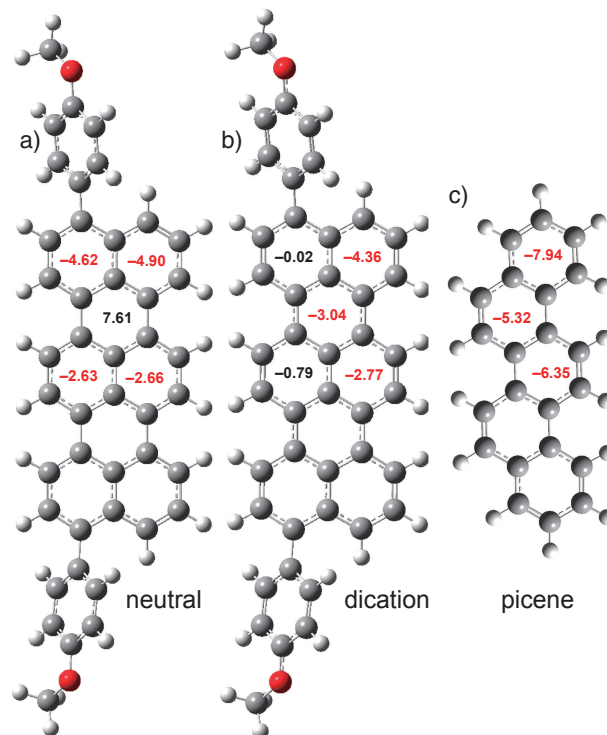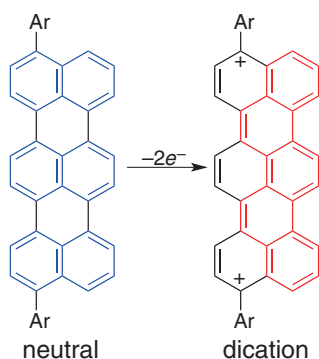

Figure 16. NICS(0) values at the selected positions of a) terrylene, b) terrylene dication, and c) picene.

Besides the polyacetylene and poly(p-phenylene) resonance forms, we suggest a polyphenacene form as a new entry of the electronic structures for polyrylenes (Figure 17d).

Scheme 4. Schematic representation of the aromaticity relocation of terrylene **4** upon the two-electron oxidation.
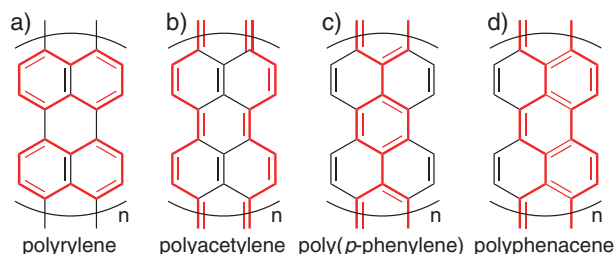

Figure 17. Conjugation representations of polyrylene.

4. Conclusions

In this article, we have analyzed the stepwise oxidation processes of the pyrene and perylene derivatives in detail via the corresponding radical cations both experimentally and theoretically.

Pyrene **1** showed a moderate fluorescence quantum yield in the solid state. No pyrene–pyrene interactions are evident in the solid state as proven by the single-crystal X-ray analysis, which may make them appealing for use in light-emitting devices.[73] The radical cation $\mathbf{1}^{\bullet+}$ showed the ESR signal and the spin density was delocalized at 1,3,6,8-positions. The dication $\mathbf{1}^{2+}$ was observed by ^{13}C NMR at low temperature. From the X-ray data of $\mathbf{1}^{2+}$, when calculating the HOMA values, it is revealed the aromatic part relocates from biphenyl unit to naphthyl part upon $2e^-$ oxidation.

Perylenes **2** and **3** also showed moderate fluorescence quantum yields in the solid state. The radical cations of diarylperylenes $\mathbf{2}^{\bullet+}$ and $\mathbf{3}^{\bullet+}$ showed the ESR signals and the spin densities were delocalized particularly at 3,4,9,10-positions. In the case of 3,9-diarylperylene **2**, we could find the anthracene structure in the doubly positive-charged conditions, while the phenanthrene skeleton appeared in two-electron oxidized 3,10-diarylperylene **3**.

We also investigated the aromaticity relocation in the larger PAH terrylene. While the electronic structure of terrylene at the neutral ground state is assumed to be the connected naphthalenes, the aromaticity of benzene rings fusing naphthalenes drastically increases upon $2e^-$ oxidation. Consequently the total aromatic structure of terrylene relocates towards that of picene. Although the theoretical calculations indicated parallel polyacetylene chains or a planar poly(p-phenylene) bridged by double bonds for polyrylenes, we illustrated a new resonance form

by polyphenacene. The way to assess the physical properties of polyrylene would be to prepare a discrete soluble derivative.[68]

References

1 G. A. Olah, *J. Org. Chem.* **2005**, *70*, 2413.

2 a) A. J. Fatiadi, *J. Org. Chem.* **1967**, *32*, 2903. b) A. C. Buchanan, III, A. S. Dworkin, G. P. Smith, *J. Am. Chem. Soc.* **1980**, *102*, 5262. c) H. Guenther, P. Kovacic, *Synth. Commun.* **1984**, *14*, 413.

3 a) O. Hammerich, V. D. Parker, *Acta Chem. Scand., Ser. B* **1982**, *36*, 519. b) B. Reitstöen, V. D. Parker, *J. Am. Chem. Soc.* **1990**, *112*, 4968.

4 S. Li, Z. Jia, K. Nakajima, K. Kanno, T. Takahashi, *J. Org. Chem.* **2011**, *76*, 9983.

5 D. Hohnholz, A. G. MacDiarmid, D. M. Sarno, W. E. Jones, Jr., *Chem. Commun.* **2001**, 2444.

6 a) Y. Li, Z. Wang, *Org. Lett.* **2009**, *11*, 1385. b) Y. Li, L. Hao, H. Fu, W. Pisula, X. Feng, Z. Wang, *Chem. Commun.* **2011**, *47*, 10088.

7 a) A. B. Nepomnyashchii, M. Bröring, J. Ahrens, A. J. Bard, *J. Am. Chem. Soc.* **2011**, *133*, 19498. b) A. Poirel, A. De Nicola, P. Retailleau, R. Ziessel, *J. Org. Chem.* **2012**, *77*, 7512.

8 a) A. Osuka, H. Shimidzu, *Angew. Chem., Int. Ed. Engl.* **1997**, *36*, 135. b) N. Aratani, A. Osuka, Y. H. Kim, D. H. Jeong, D. Kim, *Angew. Chem., Int. Ed.* **2000**, *39*, 1458. c) N. Aratani, A. Osuka, *Bull. Chem. Soc. Jpn.* **2015**, *88*, 1.

9 S. Hirabayashi, M. Omote, N. Aratani, A. Osuka, *Bull. Chem. Soc. Jpn.* **2012**, *85*, 558.

10 Crystallographic data for pyrene dimer: $C_{32}H_{18}$, $Mw = 402.46$, *orthorhombic*, space group *Pbcn* (No. 60), $a = 6.6188(8)$, $b = 9.3137(12)$, $c = 31.319(4)$ Å, $V = 1930.7(4)$ Å^3, $T = 90(2)$ K, $Z = 4$, reflections measured 10905, 2102 unique. The final R_1 was 0.0414 ($>2\sigma(I)$), and the final wR_2 on F^2 was 0.1489 (all data), GOF = 1.021. CCDC 1432442.

11 K. Yamashita, A. Nakamura, K. Sugiura, *Chem. Lett.* **2015**, *44*, 303.

12 a) R. E. Martin, T. Mäder, F. Diederich, *Angew. Chem., Int. Ed.* **1999**, *38*, 817. b) H. Nakanishi, N. Sumi, Y. Aso, T. Otsubo, *J. Org. Chem.* **1998**, *63*, 8632. c) N. Yoshida, H. Shimidzu, A. Osuka, *Chem. Lett.* **1998**, 55.

13 R. G. Hicks, *Org. Biomol. Chem.* **2007**, *5*, 1321.

14 a) T. Nishinaga, A. Wakamiya, D. Yamazaki, K. Komatsu, *J. Am. Chem. Soc.* **2004**, *126*, 3163. b) K. Komatsu, *Bull. Chem. Soc. Jpn.* **2007**, *80*, 2285.

15 a) A. Matsuura, T. Nishinaga, K. Komatsu, *J. Am. Chem. Soc.* **2000**, *122*, 10007. b) K. Komatsu, *Bull. Chem. Soc. Jpn.* **2001**, *74*, 407. c) T. Nishinaga, K. Komatsu, *Org. Biomol. Chem.* **2005**, *3*, 561.

16 E. Kayahara, T. Kouyama, T. Kato, H. Takaya, N. Yasuda,

S. Yamago, *Angew. Chem., Int. Ed.* **2013**, *52*, 13722.

17 M. R. Golder, B. M. Wong, R. Jasti, *Chem. Sci.* **2013**, *4*, 4285.

18 M. Bendikov, H. M. Duong, K. Starkey, K. N. Houk, E. A. Carter, F. Wudl, *J. Am. Chem. Soc.* **2004**, *126*, 7416.

19 a) A. Konishi, Y. Hirao, M. Nakano, A. Shimizu, E. Botek, B. Champagne, D. Shiomi, K. Sato, T. Takui, K. Matsumoto, H. Kurata, T. Kubo, *J. Am. Chem. Soc.* **2010**, *132*, 11021. b) A. Konishi, Y. Hirao, K. Matsumoto, H. Kurata, R. Kishi, Y. Shigeta, M. Nakano, K. Tokunaga, K. Kamada, T. Kubo, *J. Am. Chem. Soc.* **2013**, *135*, 1430.

20 a) Z. Sun, Q. Ye, C. Chi, J. Wu, *Chem. Soc. Rev.* **2012**, *41*, 7857. b) Z. Sun, Z. Zeng, J. Wu, *Chem.—Asian J.* **2013**, *8*, 2894. c) Z. Sun, S. Lee, K. H. Park, X. Zhu, W. Zhang, B. Zheng, P. Hu, Z. Zeng, S. Das, Y. Li, C. Chi, R.-W. Li, K.-W. Huang, J. Ding, D. Kim, J. Wu, *J. Am. Chem. Soc.* **2013**, *135*, 18229.

21 a) C. Lambert, *Angew. Chem., Int. Ed.* **2011**, *50*, 1756. b) A. Shimizu, R. Kishi, M. Nakano, D. Shiomi, K. Sato, T. Takui, I. Hisaki, M. Miyata, Y. Tobe, *Angew. Chem., Int. Ed.* **2013**, *52*, 6076. c) X. Zhu, H. Tsuji, K. Nakabayashi, S. Ohkoshi, E. Nakamura, *J. Am. Chem. Soc.* **2011**, *133*, 16342. d) E. V. Canesi, D. Fazzi, L. Colella, C. Bertarelli, C. Castiglioni, *J. Am. Chem. Soc.* **2012**, *134*, 19070. e) T. Nishinaga, M. Tateno, M. Fujii, W. Fujita, M. Takase, M. Iyoda, *Org. Lett.* **2010**, *12*, 5374. f) H. Miyoshi, S. Nobusue, A. Shimizu, I. Hisaki, M. Miyata, Y. Tobe, *Chem. Sci.* **2014**, *5*, 163.

22 a) M. Abe, *Chem. Rev.* **2013**, *113*, 7011. b) J. Casado, R. P. Ortiz, J. T. Lopez Navarrete, *Chem. Soc. Rev.* **2012**, *41*, 5672. c) M. Abe, J. Ye, M. Mishima, *Chem. Soc. Rev.* **2012**, *41*, 3808. d) M. Mas-Torrent, N. Crivillers, C. Rovira, J. Veciana, *Chem. Rev.* **2012**, *112*, 2506. e) I. Ratera, J. Veciana, *Chem. Soc. Rev.* **2012**, *41*, 303.

23 a) M. Banerjee, S. V. Lindeman, R. Rathore, *J. Am. Chem. Soc.* **2007**, *129*, 8070. b) M. Banerjee, R. Shukla, R. Rathore, *J. Am. Chem. Soc.* **2009**, *131*, 1780.

24 C. Simao, M. Mas-Torrent, V. André, M. T. Duarte, J. Veciana, C. Rovira, *Chem. Sci.* **2013**, *4*, 307.

25 a) T. Koide, K. Furukawa, H. Shinokubo, J.-Y. Shin, K. S. Kim, D. Kim, A. Osuka, *J. Am. Chem. Soc.* **2010**, *132*, 7246. b) S. Hiroto, K. Furukawa, H. Shinokubo, A. Osuka, *J. Am. Chem. Soc.* **2006**, *128*, 12380.

26 K. K. Laali, *Chem. Rev.* **1996**, *96*, 1873.

27 R. Einholz, H. F. Bettinger, *Angew. Chem., Int. Ed.* **2013**, *52*, 9818.

28 J. Dominikowska, M. Palusiak, *Phys. Chem. Chem. Phys.* **2011**, *13*, 11976.

29 a) E. Clar, R. Schoental, *Polycyclic Hydrocarbons*, Academic Press Inc., **1964**. b) E. Clar, *The Aromatic Sextet*, Wiley, New York, **1972**.

30 E. Clar, J. W. Wright, *Nature* **1949**, *163*, 921.

31 M. Solà, *Front Chem.* **2013**, *1*, 1.

32 R. Waack, *J. Chem. Educ.* **1962**, *39*, 469.

33 a) A. Matsumoto, M. Suzuki, D. Kuzuhara, J. Yuasa, T. Kawai, N. Aratani, H. Yamada, *Chem. Commun.* **2014**, *50*, 10956. b) A. Matsumoto, M. Suzuki, H. Hayashi, D. Kuzuhara, J. Yuasa, T. Kawai, N. Aratani, H. Yamada, *Chem.—Eur. J.* **2016**, *22*, 14462. c) A. Matsumoto, M. Suzuki, D. Kuzuhara, H. Hayashi, N. Aratani, H. Yamada, *Angew. Chem., Int. Ed.* **2015**, *54*, 8175.

34 M. J. Frisch, G. W. Trucks, H. B. Schlegel, G. E. Scuseria, M. A. Robb, J. R. Cheeseman, G. Scalmani, V. Barone, B. Mennucci, G. A. Petersson, H. Nakatsuji, M. Caricato, X. Li, H. P. Hratchian, A. F. Izmaylov, J. Bloino, G. Zheng, J. L. Sonnenberg, M. Hada, M. Ehara, K. Toyota, R. Fukuda, J. Hasegawa, M. Ishida, T. Nakajima, Y. Honda, O. Kitao, H. Nakai, T. Vreven, J. A. Montgomery, Jr., J. E. Peralta, F. Ogliaro, M. Bearpark, J. J. Heyd, E. Brothers, K. N. Kudin, V. N. Staroverov, T. Keith, R. Kobayashi, J. Normand, K. Raghavachari, A. Rendell, J. C. Burant, S. S. Iyengar, J. Tomasi, M. Cossi, N. Rega, J. M. Millam, M. Klene, J. E. Knox, J. B. Cross, V. Bakken, C. Adamo, J. Jaramillo, R. Gomperts, R. E. Stratmann, O. Yazyev, A. J. Austin, R. Cammi, C. Pomelli, J. W. Ochterski, R. L. Martin, K. Morokuma, V. G. Zakrzewski, G. A. Voth, P. Salvador, J. J. Dannenberg, S. Dapprich, A. D. Daniels, O. Farkas, J. B. Foresman, J. V. Ortiz, J. Cioslowski, D. J. Fox, *Gaussian09 (Revision B.01)*, Gaussian, Inc., Wallingford CT, **2010**.

35 a) M. Renz, K. Theilacker, C. Lambert, M. Kaupp, *J. Am. Chem. Soc.* **2009**, *131*, 16292. b) M. Renz, M. Kess, M. Diedenhofen, A. Klamt, M. Kaupp, *J. Chem. Theory Comput.* **2012**, *8*, 4189.

36 a) T. M. Figueira-Duarte, K. Müllen, *Chem. Rev.* **2011**, *111*, 7260. b) T. M. Figueira-Duarte, P. G. Del Rosso, R. Trattnig, S. Sax, E. J. W. List, K. Müllen, *Adv. Mater.* **2010**, *22*, 990.

37 T. Oyamada, H. Uchiuzou, S. Akiyama, Y. Oku, N. Shimoji, K. Matsushige, H. Sasabe, C. Adachi, *J. Appl. Phys.* **2005**, *98*, 074506.

38 M. Banerjee, V. S. Vyas, S. V. Lindeman, R. Rathore, *Chem. Commun.* **2008**, 1889.

39 K. K. Laali, P. E. Hansen, E. Gelerinter, J. J. Houser, *J. Org. Chem.* **1993**, *58*, 4088.

40 R. Kurata, K. Tanaka, A. Ito, *J. Org. Chem.* **2016**, *81*, 137.

41 L. Ji, R. M. Edkins, A. Lorbach, I. Krummenacher, C. Brückner, A. Eichhorn, H. Braunschweig, B. Engels, P. J. Low, T. B. Marder, *J. Am. Chem. Soc.* **2015**, *137*, 6750.

42 F. Würthner, C. Thalacker, S. Diele, C. Tschierske, *Chem.—Eur. J.* **2001**, *7*, 2245.

43 a) F. M. Winnik, *Chem. Rev.* **1993**, *93*, 587. b) G. Venkataramana, S. Sankararaman, *Org. Lett.* **2006**, *8*, 2739. c) V. de Halleux, J.-P. Calbert, P. Brocorens, J. Cornil, J.-P. Declercq, J.-L. Brédas, Y. Geerts, *Adv. Funct. Mater.* **2004**, *14*, 649. d) D. Rausch, C. Lambert, *Org. Lett.* **2006**, *8*, 5037.

44 I. B. Berlman, *J. Phys. Chem.* **1970**, *74*, 3085.

45 a) J. N. Moorthy, P. Natarajan, P. Venkatakrishnan, D.-F. Huang, T. J. Chow, *Org. Lett.* **2007**, *9*, 5215. b) Z. Zhao, S. Chen, J. W. Y. Lam, P. Lu, Y. Zhong, K. S. Wong, H. S. Kwok, B. Z. Tang, *Chem. Commun.* **2010**, *46*, 2221.

46 CCDC 1432443.

47 H.-J. Nie, C.-J. Yao, J.-Y. Shao, J. Yao, Y.-W. Zhong, *Chem.—Eur. J.* **2014**, *20*, 17454.

48 CCDC 1432434.

49 a) J. Kruszewski, T. M. Krygowski, *Tetrahedron Lett.* **1972**, *13*, 3839. b) T. M. Krygowski, *J. Chem. Inf. Comput. Sci.* **1993**, *33*, 70.

50 D. W. J. Cruickshank, *Acta Crystallogr.* **1957**, *10*, 504.

51 P. v. R. Schleyer, C. Maerker, A. Dransfeld, H. Jiao, N. J. R. v. E. Hommes, *J. Am. Chem. Soc.* **1996**, *118*, 6317.

52 T. Ishida, J. Aihara, *Phys. Chem. Chem. Phys.* **2009**, *11*, 7197.

53 a) E. C. Ashby, A. B. Goel, R. N. DePriest, H. S. Prasad, *J. Am. Chem. Soc.* **1981**, *103*, 973. b) K. Müllen, W. Huber, G. Neumann, C. Schnieders, H. Unterberg, *J. Am. Chem. Soc.* **1985**, *107*, 801.

54 P. Michel, A. Moradpour, P. Penven, L. Firlej, P. Bernier, B. Levy, S. Ravy, A. Zahab, *J. Am. Chem. Soc.* **1990**, *112*, 8285.

55 S. Nagarajan, C. Barthes, N. K. Girdhar, T. T. Dang, A.

Gourdon, *Tetrahedron* **2012**, *68*, 9371.

56 K. K. Laali, M. Tanaka, J. C. Fetzer, *J. Chem. Soc., Perkin Trans. 2* **1997**, 1315.

57 a) P. Schlichting, U. Rohr, K. Müllen, *Liebigs Ann./Recl.* **1997**, 395. b) T. Uchida, K. Kozawa, Y. Nagao, T. Misonoo, *Bull. Chem. Soc. Jpn.* **1979**, *52*, 1547. c) J.-H. Kim, C. E. Song, I.-N. Kang, W. S. Shin, D.-H. Hwang, *Chem. Commun.* **2013**, *49*, 3248.

58 A crystal structure of 3,9-dibromoperylene measured at room temperature has been reported in ref. 63b. Crystallographic data for 3,9-dibromoperylene: $C_{20}H_{10}Br_2$, $Mw = 410.11$, monoclinic, space group $P2_1/n$ (No. 14), $a = 3.8568(2)$, $b = 11.7896(7)$, $c = 15.2127(9)$ Å, $\beta = 98.7914(16)°$, $V = 683.59(7)$ Å^3, $T = 103(2)$ K, $Z = 2$, reflections measured 9351, 1251 unique. The final R_1 was 0.0720 ($>2\sigma(I)$), and the final wR_2 on F^2 was 0.1960 (all data), GOF = 1.106. CCDC 1432439.

59 CCDC 1432435.

60 CCDC 1432436.

61 CCDC 1432437.

62 CCDC 1432438. Several crystal structures of anthracene have been reported so far at various conditions. a) V. C. Sinclair, J. M. Robertson, A. M. Mathieson, *Acta Crystallogr.* **1950**, *3*, 251. b) A. M. Mathieson, J. M. Robertson, V. C. Sinclair, *Acta Crystallogr.* **1950**, *3*, 245.

63 a) S. Kummer, F. Kulzer, R. Kettner, Th. Basché, C. Tietz, C. Glowatz, C. Kryschi, *J. Chem. Phys.* **1997**, *107*, 7673. b) Y. Avlasevich, C. Kohl, K. Müllen, *J. Mater. Chem.* **2006**, *16*, 1053. c) L. Chen, C. Li, K. Müllen, *J. Mater. Chem. C* **2014**, *2*, 1938.

64 a) T. M. Halasinski, J. L. Weisman, R. Ruiterkamp, T. J. Lee, F. Salama, M. Head-Gordon, *J. Phys. Chem. A* **2003**, *107*, 3660. b) G. Malloci, C. Joblin, G. Mulas, *Astron. Astrophys.* **2007**, *462*, 627.

65 a) H. Sakaguchi, Y. Kawagoe, Y. Hirano, T. Iruka, M. Yano, T. Nakae, *Adv. Mater.* **2014**, *26*, 4134. b) A. Kimouche, M. M. Ervasti, R. Drost, S. Halonen, A. Harju, P. M. Joensuu, J. Sainio, P. Liljeroth, *Nat. Commun.* **2015**, *6*, 10177.

66 A. Bohnen, K.-H. Koch, W. Lüttke, K. Müllen, *Angew. Chem., Int. Ed. Engl.* **1990**, *29*, 525.

67 W. Xu, T.-W. Lee, *Mater. Horiz.* **2016**, *3*, 186.

68 W. Zeng, H. Phan, T. S. Herng, T. Y. Gopalakrishna, N. Aratani, Z. Zeng, H. Yamada, J. Ding, J. Wu, *Chem* **2017**, *2*, 81.

69 T. Minami, S. Ito, M. Nakano, *J. Phys. Chem. Lett.* **2012**, *3*, 2719.

70 K. Tanaka, K. Ueda, T. Koike, T. Yamabe, *Solid State Commun.* **1984**, *51*, 943.

71 J. T. Markiewicz, F. Wudl, *ACS Appl. Mater. Interfaces* **2015**, *7*, 28063.

72 a) S. Karabunarliev, L. Gherghel, K.-H. Koch, M. Baumgarten, *Chem. Phys.* **1994**, *189*, 53. b) S. Karabunarliev, M. Baumgarten, K. Müllen, N. Tyutyulkov, *Chem. Phys.* **1994**, *179*, 421. c) L. Talirz, H. Söde, J. Cai, P. Ruffieux, S. Blankenburg, R. Jafaar, R. Berger, X. Feng, K. Müllen, D. Passerone, R. Fasel, C. A. Pignedoli, *J. Am. Chem. Soc.* **2013**, *135*, 2060.

73 J.-Y. Hu, Y.-J. Pu, G. Nakata, S. Kawata, H. Sasabe, J. Kido, *Chem. Commun.* **2012**, *48*, 8434.